

Abstract

Tropospheric BrO was measured by a ground-based remote-sensing spectrometer at Halley in Antarctica, and BrO was measured by remote-sensing spectrometers in space using similar spectral regions and Differential Optical Absorption Spectroscopy (DOAS) analyses. Near-surface BrO was simultaneously measured at Halley by Chemical Ionisation Mass Spectrometry (CIMS), and in an earlier year near-surface BrO was measured at Halley over a long path by a DOAS spectrometer. During enhancement episodes, total amounts of tropospheric BrO from the ground-based remote-sensor were similar to those from space, but if we assume that the BrO was confined to the boundary layer they were very much larger than values measured by either near-surface technique. This large apparent discrepancy can be resolved if substantial amounts of BrO were in the free troposphere during most enhancement episodes. Amounts observed by the ground-based remote sensor at different elevation angles, and their formal inversions to vertical profiles, also show that much of the BrO was often in the free troposphere. This is consistent with the ~ 5 day lifetime of Bry, from the enhanced BrO observed during some Antarctic blizzards, and from aircraft measurements of BrO well above the surface in the Arctic.

1 Introduction

In spring in both polar regions, concentrations of tropospheric ozone can decrease rapidly from normal (background) values to almost zero, and remain there for periods of hours to days (Simpson et al., 2007). These tropospheric ozone depletion events (ODEs) are driven by bromine chemistry, the reactive bromine compounds (Bry) being released from the sea ice zone (e.g. Fan and Jacob, 1992; Simpson et al., 2007). The resultant Br catalytically removes ozone in a cycle involving BrO, a trace gas that can be measured by a variety of techniques.

AMTD

5, 5419–5448, 2012

Resolution of a discrepancy between remote and in-situ measurements

H. K. Roscoe et al.

Title Page

Abstract

Introduction

Conclusions

References

Tables

Figures

⏪

⏩

◀

▶

Back

Close

Full Screen / Esc

Printer-friendly Version

Interactive Discussion

Resolution of an discrepancy between remote and in-situ measurements

H. K. Roscoe et al.

Title Page

Abstract

Introduction

Conclusions

References

Tables

Figures

⏪

⏩

◀

▶

Back

Close

Full Screen / Esc

Printer-friendly Version

Interactive Discussion



The oxidising capacity of the polar troposphere is significantly altered by ODEs, during which oxidation is shifted towards control by halogen compounds. Furthermore, if the ozone-poor air can be transported to high enough altitude, or if the BrO or its aerosol sources can be transported to a high enough altitude that it continues to cause ozone depletion aloft, a small radiative effect can occur which would have a positive climate feedback (Roscoe et al., 2001).

In this paper, we discuss new remote-sensing and in-situ measurements of BrO in Antarctica, and address an important apparent discrepancy between the remote and the in-situ measurements. We compare them to other recent remote-sensing measurements and previous in-situ measurements to show that they suffer the same large apparent discrepancy. A similar potential discrepancy had been suggested from Arctic measurements by McElroy et al. (1999), who speculated that the discrepancy can be resolved if BrO is frequently present in the free troposphere. The way our new ground-based remote sensing measurements change with elevation viewing angle leads us to conclude that BrO is indeed frequently in the free troposphere in the Antarctic. This conclusion is reinforced by formal profile inversions of the new ground-based remote sensing measurements, and is consistent with recent Arctic airborne measurements.

Here we are not concerned with the detailed time-history of measurements of BrO or how they might relate to ODEs, nor to sea ice processes such as frost-flower growth. Instead we confine our attention to the differences and similarities between BrO results from the various measurement techniques and the conclusions that can be drawn.

2 Measurement techniques

Section 3 discusses Antarctic BrO results in spring from four instruments:

1. Ground-based Multiple-Axis DOAS (MAX-DOAS) spectrometer in 2007.
2. Satellite-borne spectrometer Global Ozone Monitor-2 (GOME-2) in 2007.

Resolution of an discrepancy between remote and in-situ measurements

H. K. Roscoe et al.

Title Page

Abstract

Introduction

Conclusions

References

Tables

Figures

⏪

⏩

◀

▶

Back

Close

Full Screen / Esc

Printer-friendly Version

Interactive Discussion

3. Near-surface long path in-situ DOAS spectrometer in 2004.

4. Near-surface local in-situ CIMS in 2007.

These instruments are defined and described below.

2.1 Ground-based MAX-DOAS spectrometer

5 Sunlight scattered from the sky was observed by a ground-based UV-visible spectrometer, located in Antarctica at Halley V research station (75.6° S, 26.7° W). The spectrometer was positioned on the roof of the clean air sector laboratory (CASLab, Jones et al., 2008), 1 km from the main base, to the SE where it receives minimal wind from the base and its generators.

10 The apparatus consisted of a temperature-controlled insulated box, mounted to a gearbox, motor and magnetic stops that enabled it to scan in elevation. The box contained the spectrometer, a quartz entrance lens and a motor controller, plus electronics to interface the spectrometer and motor controller to a PC inside the laboratory via USB. The box and its bulkhead connectors were sealed, and it contained drying agent
15 to keep the components and window moisture free. The box's proportional temperature controller used up to 30° W of DC power and was set at a value close to 0 °C. This power proved insufficient in stronger winds or the coldest temperatures (< −35 °C) at Halley in early spring, which was of concern because the spectral calibration and resolution of the spectrometer could shift with temperature. Laboratory tests at BIRA with another spectrometer of the same type had shown that the shifts became significantly
20 larger at temperatures much below 0 °C.

Spectra from the elevation-scanning (so-called Multiple Axis) spectrometer were analysed by Differential Optical Absorption Spectroscopy (the MAX-DOAS technique). Our apparatus was a miniaturised instrument of the Hoffman-Heidelberg design, using
25 an Ocean Optics USB-2000 spectrometer. It was set to average 1000 non-saturating spectra at each elevation angle, taking from 2 to 7 min depending on light intensity. It scanned to elevation angles 2°, 4°, 15° and 90°, the sequence being repeated every 8 to

**Resolution of an
discrepancy between
remote and in-situ
measurements**

H. K. Roscoe et al.

Title Page

Abstract

Introduction

Conclusions

References

Tables

Figures

⏪

⏩

◀

▶

Back

Close

Full Screen / Esc

Printer-friendly Version

Interactive Discussion



30 min, except only 1 in 3 sequences included 90° elevation. The field of view was 0.5°, so the surface snow could not have been seen at 2° elevation unless there were significant errors in the scan (see below). It measured at wavelengths from 337 to 481 nm with a spectral resolution of about 0.7 nm. BrO was analysed from 341 to 356 nm, an interval that includes 3 strong lines of BrO, and all of one and part of another O₄ line.

The observed spectrum also contains Fraunhofer lines from the atmosphere of the sun, which would interfere with BrO absorption lines, but because the Fraunhofer lines do not vary with time the observed spectra can be divided by a reference spectrum obtained at a high elevation to remove them. This reference spectrum also contains a small slant amount of NO₂ which by this division becomes subtracted from the actual slant amounts in the observed spectra. The amount of BrO is then found by fitting laboratory cross-sections to the ratio of observed to reference spectrum, after applying a high-pass filter in wavelength to the observed spectral ratio and the laboratory cross sections (the DOAS technique). The interfering trace gases O₃, O₄ and NO₂ are also included in the spectral fit.

Our DOAS analyses were carried out by the BIRA software suite “WinDOAS”. This does a separate calibration of wavelength for each spectrum, using the locations of Fraunhofer lines within it compared to those of a high-resolution solar spectrum by Kurucz (1984). It can also do a separate calibration of spectral response function using the widths of the Fraunhofer lines and of the trace gases, but the weak features of the trace gases in this region led to instabilities in the fits, so this software option was not selected. Hence we were careful to choose reference spectra at temperatures within 0.3 °C of each part-day of low-elevation spectra.

In MAX-DOAS geometry, the light path through the stratosphere is almost identical in a low-elevation view and the zenith view (e.g. Hönninger et al., 2004). Hence by using a spectrum of the zenith sky as a reference, the amount of stratospheric BrO is automatically subtracted from the spectrum at lower elevation. We used a zenith spectrum near noon on the same or a nearby day as a reference.

Resolution of an discrepancy between remote and in-situ measurements

H. K. Roscoe et al.

Title Page

Abstract

Introduction

Conclusions

References

Tables

Figures

⏪

⏩

◀

▶

Back

Close

Full Screen / Esc

Printer-friendly Version

Interactive Discussion



The measurements of BrO are measurements of the slant column, whereas it is the vertical column that is of greater scientific interest. The ratio of this slant path length to the vertical is known as the Air Mass Factor (AMF). Because there is no single path of scattered light, the effective slant paths through the atmosphere must be calculated by a radiative transfer code. Here we used the BIRA code “UVspec/DISORT”, with calculations that assumed all the BrO was in the lowest 200 m (see below for a discussion of this assumption). To account for the tropospheric amount in the reference spectrum, the vertical amount in each low-elevation spectrum was deduced by dividing the slant amount by (AMF(low-elevation) – AMF(zenith)), after averaging the slant columns (see Sect. 3)

Parts of the elevation scanning system (gearbox, magnet, magnetic switches to determine end-stops) were outside the temperature controlled box. During laboratory tests in a freezer at BAS, the magnet and switches were found to vary in sensitivity with temperature such that the elevation could vary by 0.5° between –45°C and 20°C. During a field campaign in summer, other scanners of the same design were found to have nominally horizontal views in error by over 1° (Roscoe et al., 2010) due to a combination of gearbox wear, hysteresis and errors during setting up. The spectrometer was mounted on a building on legs, that could be felt to sway in strong winds, and although the arrangement of legs preserved the nominal horizontal of the platform, in an earlier year a distant retro-reflector subtending 0.05° had to be re-centred on a telescope at frequent intervals. Coupled with the field of view of 0.5°, it is therefore just feasible for a view at a nominal 2° elevation to have observed part of the snow at the horizon from time to time, though this is not feasible for views at 4° and above.

2.2 Satellite-borne spectrometer GOME-2

The second Global Ozone Monitoring Experiment (GOME-2) is a UV-visible spectrometer looking downward from space to observe sunlight scattered from the atmosphere and the surface of the Earth (Munro et al., 2006). It measures from 240 to 790 nm, with a spectral resolution of 0.2 to 0.5 nm, and each day a solar spectrum is measured to

Resolution of an discrepancy between remote and in-situ measurements

H. K. Roscoe et al.

Title Page

Abstract

Introduction

Conclusions

References

Tables

Figures

⏪

⏩

◀

▶

Back

Close

Full Screen / Esc

Printer-friendly Version

Interactive Discussion

serve as a reference spectrum during spectral analysis. GOME-2 is on the Meteorological Operational satellite-A, launched in October 2006 to a sun-synchronous polar orbit with an equator crossing time of 09:30 LT on the descending node. Global coverage is achieved within three days at the equator and within one day towards the poles.

BrO is found by DOAS analysis, as for our MAX-DOAS in Sect. 2.1. The results shown below from Theys et al. (2011) fitted BrO in the range 332 to 359 nm, wider towards the UV than that of our MAX-DOAS analysis in order to cover 5 rather than 3 lines of BrO. This helps with nadir measurements from space because of the smaller slant paths than observed by a MAX-DOAS looking close to the horizon.

The analysis by Theys et al. (2011) is novel compared to earlier analyses of BrO from satellite-borne nadir sensors in that it calculates a rigorous vertical amount of tropospheric BrO. This is achieved by subtracting from the observed total BrO a climatological value stratospheric BrO, deduced from a chemistry transport model plus correlation with dynamical and chemical indicators. The remaining tropospheric BrO is then rescaled by a tropospheric AMF, which is often quite different to the stratospheric AMF that was conventionally used to calculate total BrO amounts.

2.3 Near-surface long path in-situ DOAS spectrometer

Between January 2004 and February 2005, the concentration of BrO was measured at Halley by a spectrometer observing a lamp via a distant retro-reflector (Saiz-Lopez et al., 2007). Light from the xenon lamp in the CASLab was reflected back to the telescope and spectrometer by an array of quartz corner cubes at a distance of 4 km. The resulting 8 km sample path was at a height of 4 to 5 m above the snowpack. Spectra between 324 and 338 nm were analysed for BrO by the DOAS method described in Sect. 2.1. This interval is at shorter wavelengths than that of our MAX-DOAS because of the larger ratio of UV to visible light from the xenon lamp compared to scattered sunlight.

2.4 Near-surface local in-situ CIMS

The Chemical Ionisation Mass Spectrometer (CIMS) at Halley was based on the method outlined by Huey et al. (1998) and Slusher et al. (2001), and the wider chemical interpretation of the results are discussed by Buys et al. (2012). The components are an inlet, a reaction chamber, a collisional dissociation chamber, an octopole ion guide plus quadrupole mass spectrometer, and an ion detector. SF₆ is converted to SF₆⁻ as it passes through an ion source, then mixed with ambient air to react with various trace gases including SO₂ and BrO. The resultant ions are detected one at a time by the mass spectrometer.

A major problem for this technique is interference by water vapour. In a high water environment, water clusters form around the reagent ion, and it is difficult to measure trace gases at concentrations of a few pptv. However, laboratory and field results (Slusher et al., 2001) indicate that at frost points below -25 °C the interference is small. No observable water interference was found at Halley during spring.

At Halley, ambient air was continually sampled at a high flow rate via a Teflon cap and wide aluminium pipe, 5 m above the snow surface. Air from the centre of the pipe was sub-sampled through a heated PFA inlet. The CIMS was operated alternately in two different modes, being switched from one to the other every few weeks:

- a. At high pressure, measuring OH and peroxy radicals.
- b. At low pressure, measuring trace gases including BrO.

In the low pressure mode, the measurement sequence consisted of integrating the signals sequentially at the various masses corresponding to the wanted ion products, including 95 amu for BrO⁻. The sequence was repeated at least every 10 s.

Sensitivity to SO₂ was found by introducing a certified standard for 1 min every two hours, those of the halogen compounds relative to SO₂ having been previously determined in the laboratory (Slusher et al., 2004). The zero of the measurement was

Resolution of a discrepancy between remote and in-situ measurements

H. K. Roscoe et al.

Title Page

Abstract

Introduction

Conclusions

References

Tables

Figures

⏪

⏩

◀

▶

Back

Close

Full Screen / Esc

Printer-friendly Version

Interactive Discussion

obtained by filtering the inlet air through activated charcoal, together with dried nylon and glass wool that had been previously soaked in NaHCO_3 solution.

3 Results

The calculation of AMF with MAX-DOAS geometry is much more difficult with high aerosol loading or significant clouds. Fortunately, high aerosol loading is rare in unpolluted Antarctica, though fog and wind-blown snow are common. We eliminated cloudy days and cloudy parts of days by choosing only portions with less than or equal to 3 oktas cloud, taken from the meteorological log at Halley. In dense cloud over highly-reflecting snow, the scattering between cloud and snow renders the light fully diffuse so that all elevations see the same scene. The diffuseness occurs at all wavelengths so that the phenomenon must affect the observed O_4 as well as the BrO , and means that the differences in O_4 between low-elevation and 90° -elevation (i.e. the O_4 signals used here) become very small in dense cloud. Hence we could use the size of the O_4 signals to interpolate cloudiness between the 3-hourly meteorological observations. Such cloudy periods were assessed by eye and eliminated. With one day's exception, we also eliminated observations closer to twilight than a solar zenith angle of 85° , because the stratospheric amount can then differ markedly from that of the noon reference as the interference from stratospheric ozone then becomes very large, and because light intensity then becomes much less. The exception was 25 August, a day early in the season when the CIMS was already operating, and with some completely clear skies – eliminating solar zenith angles of less than 85° would have left almost no data on this day. Periods with rapidly changing spectrometer temperatures were also eliminated for the technical reasons discussed in Sect. 2.1.

Figure 1 shows two days of measurements of slant amounts, chosen to represent those with larger amounts of cloud (12 October) and smaller amounts of cloud (13 October). Important features are:

Resolution of an discrepancy between remote and in-situ measurements

H. K. Roscoe et al.

Title Page

Abstract

Introduction

Conclusions

References

Tables

Figures



Back

Close

Full Screen / Esc

Printer-friendly Version

Interactive Discussion



Resolution of an discrepancy between remote and in-situ measurements

H. K. Roscoe et al.

Title Page

Abstract

Introduction

Conclusions

References

Tables

Figures

⏪

⏩

◀

▶

Back

Close

Full Screen / Esc

Printer-friendly Version

Interactive Discussion

- a. There is less O₄ on 12 October, because there was more cloud.
- b. Despite using same-day reference spectra for each of the two days, the noise on 12 October is larger. We suspect this is due to the variability of the larger cloud amounts.
- c. The noise is large enough that some averaging must be done – working with individual elevation scans is not realistic. We chose to use daily medians (see below).
- d. All slant amounts have a tendency to increase with increasing solar zenith angle. This is probably because of interference from stratospheric ozone, not properly accounted for in the spectral inversions, as well as from stratospheric BrO. If they are from stratospheric gases, they should be identical at all elevations and so be removed by the subtraction of zenith amounts.

Figure 2 shows the total vertical tropospheric BrO measured by the MAX-DOAS on the sunny days or part-days, averaged over the three elevations observed, after subtracting the slant amount in the zenith view and dividing by the difference in AMF from that of the zenith view. This calculation used the median of each day's or part-day's slant columns – we chose median rather than mean because there were some obvious spikes in the raw time series of slant columns (not seen in the days in Fig. 1), presumably due to data drop out, and medians are the simplest way of reducing sensitivity to spikes in data. Drop out was probably because of difficulties with the USB link to the computer, which had to be rebooted frequently until a USB connector on the moving part of the elevation scan was relocated part way through the year.

Although the MAX-DOAS measured BrO from 25 August 2007 until 5 February 2008, in Fig. 2 we show just the period in spring 2007 that overlaps the simultaneous CIMS measurements, plus the following month to illustrate the continuing quality and features of the data. From Fig. 2, we see that the ground-based MAX-DOAS spectrometer apparently observed from 0 to 5×10^{13} molec cm⁻² of tropospheric BrO above Halley in spring 2007.

from 75 to 300 m, with a mean of 140 m. Three of the days also had another layer discernible just above ground clutter, varying in height from 25 to 40 m. To proceed with the comparison, we chose a layer thickness of 200 m as a starting point.

Assuming the value of 200 m, the MAX-DOAS vertical column would become 130 pptv on 6 September 2007. This is at least 10 times the BrO observed in-situ by CIMS. The scaling is inversely proportional to layer thickness, so a layer thickness of 2000 m would be needed to obtain good agreement. Figure 4 compares CIMS results to MAX-DOAS assuming a boundary layer height of 200 m but dividing MAX-DOAS results by 10, to demonstrate the consistency of the discrepancy. Choosing a layer thickness equal to the mean sodar value of 140 m, or equal to that of the lower secondary layer seen by sodar on some days, would make the disagreement worse.

A similar calculation was made by Wagner et al. (2007) for MAX-DOAS measurements of BrO enhancements from a ship in the Weddell Sea in 2006. Their Table 1 converts a slant column of 10^{15} molec cm^{-2} at 1° elevation to 50 pptv in a boundary layer of thickness 200 m. Our slant column difference from 90° at 2° elevation on 6 September was 0.8×10^{15} molec cm^{-2} , which at 1° elevation would be a slant column difference of about 1.5×10^{15} molec cm^{-2} , and our result is 130 pptv. This is a slightly larger conversion factor than that derived by Wagner et al. (2007), but the difference is small compared to the discrepancy shown in Fig. 4. Although Wagner et al. (2007) noted that their MAX-DOAS measurements were equivalent to unrealistically large boundary-layer BrO mixing ratios, they refrained from suggesting that there was in fact a discrepancy.

The potential for the discrepancy was strongly suggested by McElroy et al. (1999) from airborne measurements over the central Arctic Ocean in spring. They observed similarly large vertical column densities of BrO, which led them to speculate that much of the BrO must be in the free troposphere, and that lofting of boundary layer air was indeed likely via convection due to water leads. However, there were no simultaneous in-situ measurements to confirm the discrepancy, and no geometrical considerations in the measurements to confirm that BrO was present at higher altitudes.

Resolution of an discrepancy between remote and in-situ measurements

H. K. Roscoe et al.

Title Page

Abstract

Introduction

Conclusions

References

Tables

Figures

⏪

⏩

◀

▶

Back

Close

Full Screen / Esc

Printer-friendly Version

Interactive Discussion



Resolution of an discrepancy between remote and in-situ measurements

H. K. Roscoe et al.

Title Page

Abstract

Introduction

Conclusions

References

Tables

Figures

⏪

⏩

◀

▶

Back

Close

Full Screen / Esc

Printer-friendly Version

Interactive Discussion



Because of its remote-sensing geometry, MAX-DOAS observes up to several km away from its site, so our simultaneous comparison with in-situ results could be rendered void on days when winds were light so that air masses travelled slowly. However, on 5 of the 9 days for which there are simultaneous MAX-DOAS and CIMS results, Fig. 4 shows that CIMS results are a maximum (i.e. closest to MAX-DOAS) at the times of the MAX-DOAS measurements. Hence the discrepancy would be larger if the air sampled by CIMS was observed by MAX-DOAS up to 2 h earlier or later.

The inescapable conclusion is that large amounts of BrO must frequently lie above 200 m during observations of Antarctic enhancement episodes at near-coastal sites such as Halley, and from Wagner et al. (2007) over the sea ice zone – much of the BrO must usually be in the free troposphere.

The conclusion is borne out by the variation of the MAX-DOAS vertical and slant columns with elevation angle. Figure 5 shows that the vertical column appears much larger at 15° elevation angle than at 2° or 4° on most days in spring with enhanced BrO, in excess of the approximate errors. This is only possible if the AMFs are incorrect and much of the BrO in fact lies above 200 m.

The calculation of approximate errors is problematic. In fact there is no formal error for the median of a data set, unlike for the mean. We determined standard deviations of each day's slant columns, and looked at their minima, on the assumption that the scatter of the points excluding outliers (the effect of the median being to exclude outliers) would be represented by this minimum standard deviation. These minima were similar at each elevation, as expected, so we adopted their mean and derived the standard error by dividing by the square root of the number of data points, which differed significantly from day to day because of elimination of cloudy parts of days. These errors are then only the random component, systematic errors are not included.

Figure 6 shows the slant columns from which the vertical columns are deduced, in which the slant columns are smallest at highest elevation, as expected. Figure 6 also shows that some days with non-zero cloud amounts produce smaller O₄ slant columns, because multiple scattering between cloud and snow can make all elevations view a

similar scene. If we were to attempt to compensate for this in the BrO columns, the vertical amounts of BrO would increase, again making the discrepancy from the in-situ sensor worse.

5 Vertical profile inversion of MAX-DOAS data

AMFs at the different MAX-DOAS elevation angles have different sensitivities to absorbers at different heights. The higher the altitude of the absorber, the more similar are the AMFs, whereas for an absorber close to the surface, low elevations have much larger AMFs than those for high elevations.

This property can be used to invert a vertical profile of a set of MAX-DOAS measurements. We used the Bremen scheme detailed in Wittrock (2006), which includes optimal estimation (Rodgers et al., 1990). This scheme simultaneously fits to the O₄ and BrO measurements, as scattering by aerosol or thin-cloud, which strongly affects O₄ amounts, is an important part of the calculation. The inputs to the scheme are the solar zenith and azimuth angles, as well as the slant amounts of BrO and O₄ plus their random errors. The errors allow a calculation of the formal random error component of the inverted profile.

The inversion results in Fig. 7 show that many profiles have significant amounts above the lowest layers. The Trace of the averaging kernel, widely used as measure of the number of pieces of independent information in the profiles (Rodgers et al., 1990), has a mean value of 2.5, and in Fig. 7 we have assumed 3 pieces of information.

The averaging kernels (not shown) demonstrate that the value in the lowest 300 to 500 m is one of these independent pieces of information, so we have used the mean inverted mixing ratio over the lowest 400 m as a measure of the near-surface mixing ratio for comparison with CIMS data. Figure 8 shows the results, which are much more convincing than those of Fig. 4. There is still disagreement in Fig. 8, which is to be expected as the vertical inversion cannot say whether there is less or more BrO at 10 m than at 300 m.

Resolution of a discrepancy between remote and in-situ measurements

H. K. Roscoe et al.

Title Page

Abstract

Introduction

Conclusions

References

Tables

Figures

◀

▶

◀

▶

Back

Close

Full Screen / Esc

Printer-friendly Version

Interactive Discussion



**Resolution of an
discrepancy between
remote and in-situ
measurements**H. K. Roscoe et al.

[Title Page](#)[Abstract](#)[Introduction](#)[Conclusions](#)[References](#)[Tables](#)[Figures](#)[⏪](#)[⏩](#)[◀](#)[▶](#)[Back](#)[Close](#)[Full Screen / Esc](#)[Printer-friendly Version](#)[Interactive Discussion](#)

The total vertical column from the inversion program should be a better measure of total column than any of those from the slant columns at individual elevation angles (Fig. 5) or their mean (Fig. 2). The slant column at 15° elevation is the least dependent on the profile shape, but it still has some dependency. Figure 9 shows that the vertical columns from the inversion program range up to 8×10^{13} molec cm⁻². This is only slightly larger than the upper limit of 7×10^{13} molec cm⁻² from GOME-2 near Halley in spring 2007 (Theys et al., 2011).

The profiles in Fig. 7 showing significant amounts of BrO above 1 km are in contrast to inversions of similar measurements at the Arctic coast (Barrow) in spring 2009 (Friess et al., 2011). Their Fig. 13 shows some enhancements at 0.2 km relative to near-surface values, but very little above 0.5 km. Similarly, in the Arctic near Alert in spring 2000, Honninger et al. (2002) deduced little uplift of enhanced BrO beyond 1 km; and in order to compare BrO measurements in the Arctic Ocean in spring 2008, Nghiem et al. (2012) calculated uplift from trajectories, showing that none exceeded 500 m.

These results suggest somewhat different meteorological conditions in various regions of the Arctic in spring.

6 Conclusions

There is a large discrepancy between remote-sensing and in-situ measurements of BrO during Antarctic enhancements episodes if the BrO is assumed to lie within a surface layer similar in thickness to that of the boundary layer. Possible sources of error identified in analysis of the MAX-DOAS results would make the disagreement worse. The measurements can only be reconciled if large amounts of BrO are frequently at higher altitudes (i.e. in the free troposphere). The change of MAX-DOAS results with elevation angle supports this conclusion. Formal inversion of vertical profiles of MAX-DOAS BrO also shows large amounts at higher altitudes, and the resulting near-surface mixing ratios are of similar magnitude to the CIMS surface mixing ratios. Hence we

conclude that large amounts of BrO frequently extend to several km altitude during Antarctic enhancement episodes.

Perhaps we should not be surprised at this conclusion. BrO enhancements are often observed during storms, with surface winds that can exceed 15 m s^{-1} (Jones et al., 2009). This must stir the atmosphere so vigorously that air must be lofted several km. Furthermore, Fig. 10 illustrates that:

- a. Many ozone depletion episodes show ozone loss in the free troposphere (Roscoe et al., 2001; Jones et al., 2010), sometimes with back-trajectories that saw the surface 3 to 5 days earlier (Roscoe et al., 2001), and the lifetime of BrO in the absence of precipitation is 3 to 5 days (Yang et al., 2010).
- b. At least one of several flights measuring BrO from an aircraft during an Arctic campaign in 2008 (Fig. 10, right hand panel) observed enhanced BrO in a layer from 1.5 to 2.5 km (Salawitch et al., 2010; Choi et al., 2012).

We conclude that the large apparent discrepancy between surface measurements of BrO mixing ratio and remote-sensing measurements of BrO vertical columns during enhancement episodes in Antarctica is resolved by BrO being routinely present well above the surface during such episodes. This conclusion is consistent with other aspects of the remote-sensing measurements, and with other observations of BrO enhancement episodes.

Acknowledgements. This study is part of the British Antarctic Survey's Polar Science for Planet Earth programme, funded by the Natural Environment Research Council. We thank Caroline Fayt and Gaia Pinardi of BIRA for help with running WinDOAS code on the specific output from our MAX-DOAS spectrometer, and Francois Hendrick of BIRA for running the AMF code. We also thank Udo Friess and Thomas Wagner for useful discussions on MAX-DOAS data. Finally, we thank Steve Colwell and Phil Anderson of BAS for providing Halley meteorological and sodar data, respectively.

Resolution of an discrepancy between remote and in-situ measurements

H. K. Roscoe et al.

Title Page

Abstract

Introduction

Conclusions

References

Tables

Figures

⏪

⏩

◀

▶

Back

Close

Full Screen / Esc

Printer-friendly Version

Interactive Discussion



References

- Anderson, P. S. and Neff, W. D.: Boundary layer physics over snow and ice, *Atmos. Chem. Phys.*, 8, 3563–3582, doi:10.5194/acp-8-3563-2008, 2008.
- 5 Buys, Z., Brough, N., Huey, G., Tanner, D., von Glasow, R., and Jones, A. E.: Br₂, BrCl, BrO and surface ozone in coastal Antarctica: a meteorological and chemical analysis, *Atmos. Chem. Phys. Discuss.*, 12, 11035–11077, doi:10.5194/acpd-12-11035-2012, 2012.
- Choi, S., Wang, Y., Salawitch, R. J., Canty, T., Joiner, J., Zeng, T., Kurosu, T. P., Chance, K., Richter, A., Huey, L. G., Liao, J., Neuman, J. A., Nowak, J. B., Dibb, J. E., Weinheimer, A. J., Diskin, G., Ryerson, T. B., da Silva, A., Curry, J., Kinnison, D., Tilmes, S., and Levelt, P. F.: Analysis of satellite-derived Arctic tropospheric BrO columns in conjunction with aircraft measurements during ARCTAS and ARCPAC, *Atmos. Chem. Phys.*, 12, 1255–1285, doi:10.5194/acp-12-1255-2012, 2012.
- 10 Fan, S. M. and Jacob, D. J.: Surface ozone depletion in Arctic spring sustained by bromine reactions on aerosols, *Nature*, 359, 522–524, 1992.
- 15 Friess, U., Sihler, H., Sander, R., Pöhler, D., Yilmaz, S., and Platt, U.: The vertical distribution of BrO and aerosols in the Arctic: Measurements by active and passive differential optical absorption spectroscopy, *J. Geophys. Res.*, 116, D00R04, doi:10.1029/2011JD015938, 2011.
- Hönninger, G. and Platt, U.: Observations of BrO and its vertical distribution during surface ozone depletion at Alert, *Atmos. Environ.*, 36, 2481–2489, 2002.
- 20 Hönninger, G., von Friedeburg, C., and Platt, U.: Multi axis differential optical absorption spectroscopy (MAX-DOAS), *Atmos. Chem. Phys.*, 4, 231–254, doi:10.5194/acp-4-231-2004, 2004.
- Huey, L. G., Dunlea, E. J., Lovejoy, E. R., Hanson, D. R., Norton, R. B., Fehsenfeld, F. C., and Howard, C. J.: Fast time response measurements of HNO₃ in air with a chemical ionization mass spectrometer, *J. Geophys. Res.*, 103, 3355–3360, 1998.
- 25 Jones, A. E., Wolff, E. W., Salmon, R. A., Bauguitte, S. J.-B., Roscoe, H. K., Anderson, P. S., Ames, D., Clemitshaw, K. C., Fleming, Z. L., Bloss, W. J., Heard, D. E., Lee, J. D., Read, K. A., Hamer, P., Shallcross, D. E., Jackson, A. V., Walker, S. L., Lewis, A. C., Mills, G. P., Plane, J. M. C., Saiz-Lopez, A., Sturges, W. T., and Worton, D. R.: Chemistry of the Antarctic Boundary Layer and the Interface with Snow: an overview of the CHABLIS campaign, *Atmos. Chem. Phys.*, 8, 3789–3803, doi:10.5194/acp-8-3789-2008, 2008.
- 30

Resolution of an discrepancy between remote and in-situ measurements

H. K. Roscoe et al.

Title Page

Abstract

Introduction

Conclusions

References

Tables

Figures

◀

▶

◀

▶

Back

Close

Full Screen / Esc

Printer-friendly Version

Interactive Discussion



**Resolution of an
discrepancy between
remote and in-situ
measurements**

H. K. Roscoe et al.

Title Page

Abstract

Introduction

Conclusions

References

Tables

Figures

◀

▶

◀

▶

Back

Close

Full Screen / Esc

Printer-friendly Version

Interactive Discussion

- Jones, A. E., Anderson, P. S., Begoin, M., Brough, N., Hutterli, M. A., Marshall, G. J., Richter, A., Roscoe, H. K., and Wolff, E. W.: BrO, blizzards, and drivers of polar tropospheric ozone depletion events, *Atmos. Chem. Phys.*, 9, 4639–4652, doi:10.5194/acp-9-4639-2009, 2009.
- Jones, A. E., Anderson, P. S., Wolff, E. W., Roscoe, H. K., Marshall, G. J., Richter, A., Brough, N., and Colwell, S. R.: Vertical structure of Antarctic tropospheric ozone depletion events: characteristics and broader implications, *Atmos. Chem. Phys.*, 10, 7775–7794, doi:10.5194/acp-10-7775-2010, 2010.
- Kurucz, R. L., Furenlid, I., Brault, J., and Testerman, L.: Solar flux atlas from 296 nm to 1300 nm, National Solar Observatory Atlas No. 1, 1984.
- Liao, J., Sihler, H., Huey, L. G., Neuman, J. A., Tanner, D. J., Friess, U., Platt, U., Flocke, F. M., Orlando, J. J., Shepson, P. B., Beine, H. J., Weinheimer, A. J., Sjostedt, S. J., Nowak, J. B., Knapp, D. J., Staebler, R. M., Zheng, W., Sander, R., Hall, S. R., and Ullmann, K.: A comparison of Arctic BrO measurements by chemical ionisation mass spectrometry and long path-differential optical absorption spectroscopy, *J. Geophys. Res.*, 116, D00R02, doi:10.1029/2010JD014788, 2011.
- McElroy, C. T., McLinden, C. A., and McConnell, J. C.: Evidence for bromine monoxide in the free troposphere during the Arctic polar sunrise, *Nature*, 397, 338–340, 1999.
- Munro, R., Eisinger, M., Anderson, C., Callies, J., Corpaccioli, E., Lang, R., Lefebvre, A., Livschitz, Y., and Pérez Albiñana, A.: GOME-2 on Metop: From in-orbit verification to routine operations, in: *The 2006 EUMETSAT Meteorological Satellite Conference*, 12–16 June, 8711, p. 48, Helsinki, Finland, 2006.
- Nghiem, S. V., Rigor, I. G., Richter, A., Burrows, J. P., Shepson, P. B., Bottenheim, J., Barber, D. G., Steffen, A., Latonas, Wang, F., Stern, G., Clemente-Colon, P., Martin, S., Hall, D. K., Kaleschke, L., Tackett, P., Neumann, G., and Asplin, M. G.: Field and satellite observations of the formation and distribution of Arctic atmospheric bromine above a rejuvenated sea ice cover, *J. Geophys. Res.*, 117, D00S05, doi:10.1029/2011JD016268, 2012.
- Rodgers, C. D.: Characterization and Error Analysis of Profiles Retrieved From Remote Sounding Measurements, *J. Geophys. Res.*, 95, 5587–5595, 1990.
- Roscoe, H. K., Kreher, K., and Friess, U.: Ozone loss episodes in the free Antarctic troposphere, suggesting a possible climate feedback, *Geophys. Res. Lett.*, 28, 2911–2914, 2001.
- Roscoe, H. K., Van Roozendaal, M., Fayt, C., du Piesanie, A., Abuhassan, N., Adams, C., Akrami, M., Cede, A., Chong, J., Clémer, K., Friess, U., Gil Ojeda, M., Goutail, F., Graves, R., Griesfeller, A., Grossmann, K., Hemerijckx, G., Hendrick, F., Herman, J., Hermans, C., Irie,

**Resolution of an
discrepancy between
remote and in-situ
measurements**

H. K. Roscoe et al.

[Title Page](#)[Abstract](#)[Introduction](#)[Conclusions](#)[References](#)[Tables](#)[Figures](#)[⏪](#)[⏩](#)[◀](#)[▶](#)[Back](#)[Close](#)[Full Screen / Esc](#)[Printer-friendly Version](#)[Interactive Discussion](#)

H., Johnston, P. V., Kanaya, Y., Kreher, K., Leigh, R., Merlaud, A., Mount, G. H., Navarro, M., Oetjen, H., Pazmino, A., Perez-Camacho, M., Peters, E., Pinardi, G., Puentedura, O., Richter, A., Schönhardt, A., Shaiganfar, R., Spinei, E., Strong, K., Takashima, H., Vlemmix, T., Vrekoussis, M., Wagner, T., Wittrock, F., Yela, M., Yilmaz, S., Boersma, F., Hains, J., Kroon, M., Piters, A., and Kim, Y. J.: Intercomparison of slant column measurements of NO₂ and O₄ by MAX-DOAS and zenith-sky UV and visible spectrometers, *Atmos. Meas. Tech.*, 3, 1629–1646, doi:10.5194/amt-3-1629-2010, 2010.

Saiz-Lopez, A., Mahajan, A. S., Salmon, R. A., Bauguitte, S. J.-B., Jones, A. E., Roscoe, H. K., and Plane, J. M. C.: Boundary layer halogens in coastal Antarctica, *Science*, 317, 348–351, 2007.

Salawitch, R. J., Canty, T., Kurosu, T., Chance, K., Liang, Q., da Silva, A., Pawson, S., Nielsen, J. E., Rodriguez, J. M., Bhartia, P. K., Liu, X., Huey, L. G., Liao, J., Stickel, R. E., Tanner, D. J., Dibb, J. E., Simpson, W. R., Donohoue, D., Weinheimer, A., Flocke, F., Knapp, D., Montzka, D., Neuman, J. A., Nowak, J. B., Ryerson, T. B., Oltmans, S., Blake, D. R., Atlas, E. L., Kinnison, D. E., Tilmes, S., Pan, L. L., Hendrick, F., Van Roozendaal, M., Kreher, K., Johnston, P. V., Gao, R. S., Johnson, B., Bui, T. P., Chen, G., Pierce, R. B., Crawford, J. H., and Jacob, D. J.: A new interpretation of total column BrO during Arctic spring, *Geophys. Res. Lett.*, 37, L21805, doi:10.1029/2010GL043798, 2010.

Simpson, W. R., von Glasow, R., Riedel, K., Anderson, P., Ariya, P., Bottenheim, J., Burrows, J., Carpenter, L. J., Frieß, U., Goodsite, M. E., Heard, D., Hutterli, M., Jacobi, H.-W., Kaleschke, L., Neff, B., Plane, J., Platt, U., Richter, A., Roscoe, H., Sander, R., Shepson, P., Sodeau, J., Steffen, A., Wagner, T., and Wolff, E.: Halogens and their role in polar boundary-layer ozone depletion, *Atmos. Chem. Phys.*, 7, 4375–4418, doi:10.5194/acp-7-4375-2007, 2007.

Slusher, D. L., Pitteri, J., Haman, B. J., Tanner, D. J., and Huey, L. G.: A chemical ionization technique for measurement of Pernitric Acid in the upper troposphere and the Polar Boundary layer, *Geophys. Res. Lett.*, 28, 3875–3878, 2001.

Slusher, D. L., Tanner, D. J., Flocke, F. M., and Roberts, J. M.: A thermal dissociation chemical ionization mass spectrometry (TD-CIMS) technique for the simultaneous measurement of peroxyacyl nitrates and dinitrogen pentoxide, *J. Geophys. Res.*, 109, doi:10.1029/2004JD004670, 2004.

Theys, N., Van Roozendaal, M., Hendrick, F., Yang, X., De Smedt, I., Richter, A., Begoin, M., Errera, Q., Johnston, P. V., Kreher, K., and De Mazière, M.: Global observations of tropo-

**Resolution of an
discrepancy between
remote and in-situ
measurements**

H. K. Roscoe et al.

[Title Page](#)[Abstract](#)[Introduction](#)[Conclusions](#)[References](#)[Tables](#)[Figures](#)[⏪](#)[⏩](#)[◀](#)[▶](#)[Back](#)[Close](#)[Full Screen / Esc](#)[Printer-friendly Version](#)[Interactive Discussion](#)

spheric BrO columns using GOME-2 satellite data, Atmos. Chem. Phys., 11, 1791–1811, doi:10.5194/acp-11-1791-2011, 2011.

Wagner, T., Ibrahim, O., Sinreich, R., Frieß, U., von Glasow, R., and Platt, U.: Enhanced tropospheric BrO over Antarctic sea ice in mid winter observed by MAX-DOAS on board the research vessel Polarstern, Atmos. Chem. Phys., 7, 3129–3142, doi:10.5194/acp-7-3129-2007, 2007.

Wittrock, F.: The retrieval of oxygenated volatile organic compounds by remote sensing techniques, PhD thesis, University of Bremen, May 2006, available at: <http://nbn-resolving.de/urn:nbn:de:gbv:46-diss000104818> (last access: 26 July 2012), 2006.

Yang, X., Pyle, J. A., Cox, R. A., Theys, N., and Van Roozendaal, M.: Snow-sourced bromine and its implications for polar tropospheric ozone, Atmos. Chem. Phys., 10, 7763–7773, doi:10.5194/acp-10-7763-2010, 2010.

Resolution of an discrepancy between remote and in-situ measurements

H. K. Roscoe et al.

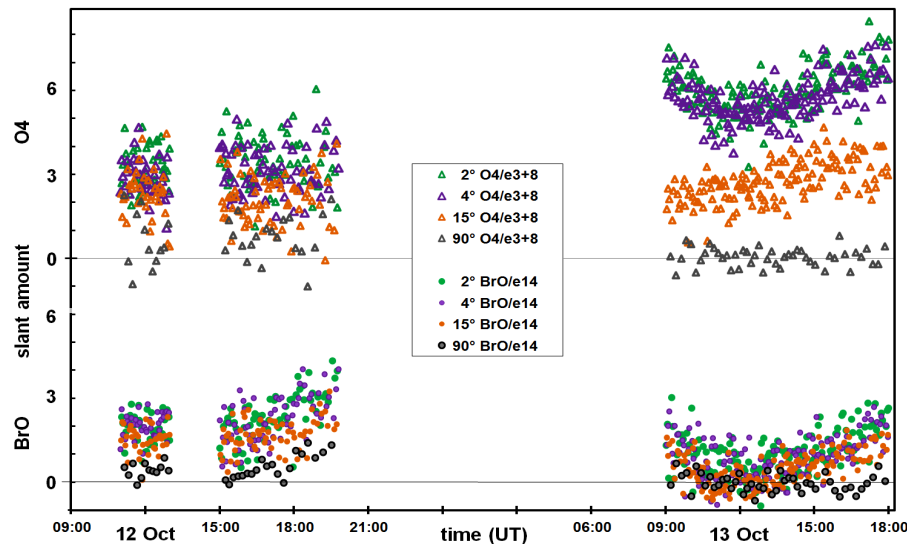


Fig. 1. Individual measurements by MAX-DOAS at Halley in 2007, on two selected days, at the 4 angles of the elevation scan. The lower half shows slant amounts of BrO (units 10^{14} molec cm^{-2}); the upper half shows slant amounts of O_4 (units 10^3 molec 2 cm^{-4}). 12 October had more cloud, hence the larger amounts of O_4 (see text); and the cloud was more variable, hence the larger scatter.

[Title Page](#)[Abstract](#)[Introduction](#)[Conclusions](#)[References](#)[Tables](#)[Figures](#)[◀](#)[▶](#)[◀](#)[▶](#)[Back](#)[Close](#)[Full Screen / Esc](#)[Printer-friendly Version](#)[Interactive Discussion](#)

Resolution of an discrepancy between remote and in-situ measurements

H. K. Roscoe et al.

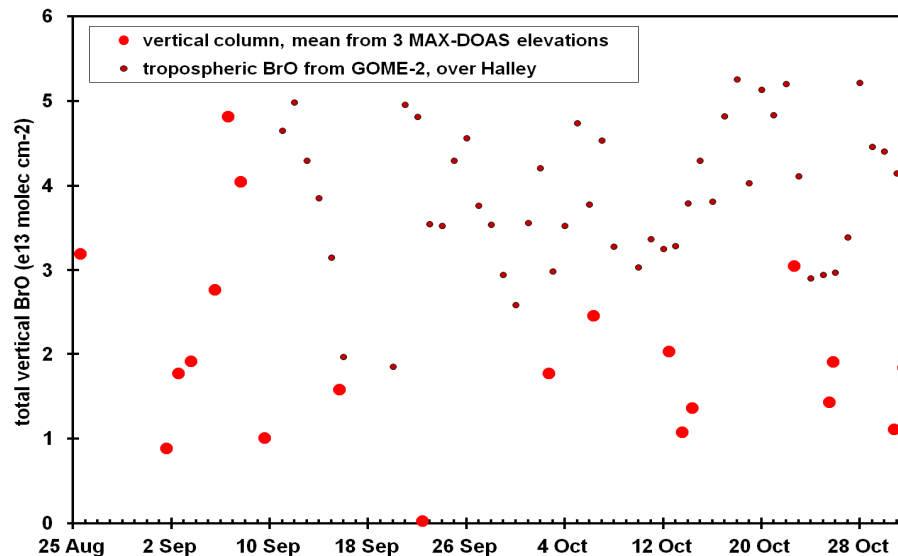


Fig. 2. Total vertical tropospheric BrO at Halley in Antarctica in spring 2007. Large red circles: measured by our MAX-DOAS, these are medians of measurements on each sunny day or part-day (≤ 3 oktas), and are the mean of measurements at elevations of 2°, 4° and 15°. Small red circles with black rims: GOME-2 data within 200 km of Halley (courtesy Nicholas Theys, see Theys et al., 2011).

[Title Page](#)[Abstract](#)[Introduction](#)[Conclusions](#)[References](#)[Tables](#)[Figures](#)[⏪](#)[⏩](#)[◀](#)[▶](#)[Back](#)[Close](#)[Full Screen / Esc](#)[Printer-friendly Version](#)[Interactive Discussion](#)

Resolution of an discrepancy between remote and in-situ measurements

H. K. Roscoe et al.

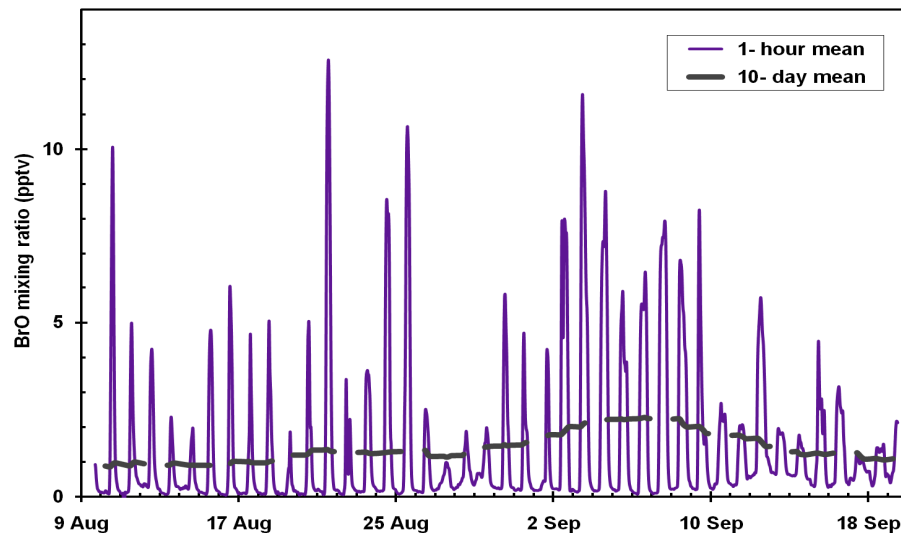


Fig. 3. Measurements of BrO by the CIMS in-situ sampler at Halley in spring 2007. The solid purple line is the 10-min data smoothed by a triangular function of half-width 1 h. The thick grey dashed line is a 10-day running mean of all values, including night-time for ease of comparison with data from Saiz-Lopez et al. (2007), and between 10 August and 19 September its value was between 1 and 2.2 pptv.

[Title Page](#)[Abstract](#)[Introduction](#)[Conclusions](#)[References](#)[Tables](#)[Figures](#)[⏪](#)[⏩](#)[◀](#)[▶](#)[Back](#)[Close](#)[Full Screen / Esc](#)[Printer-friendly Version](#)[Interactive Discussion](#)

Resolution of an discrepancy between remote and in-situ measurements

H. K. Roscoe et al.

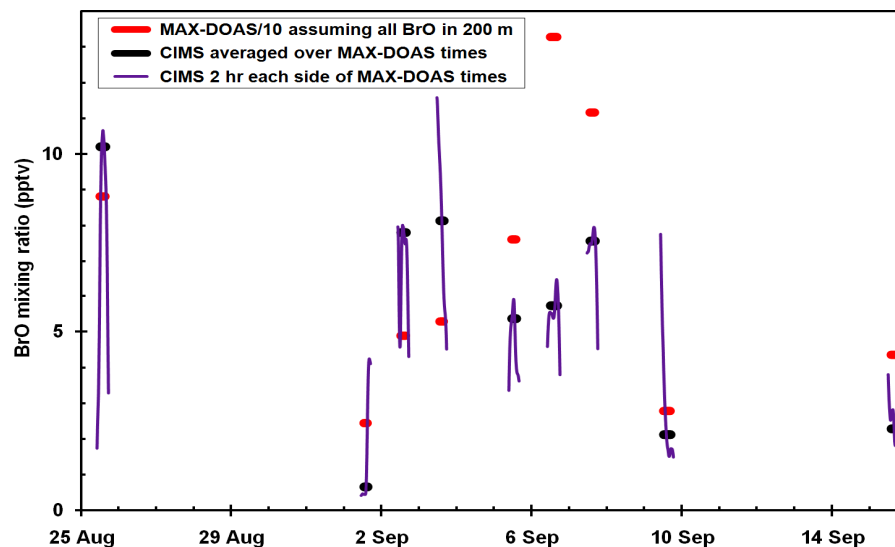


Fig. 4. Medians of each sunny day or part-day of MAX-DOAS BrO, divided by 10 and assuming all BrO is confined to a surface layer of thickness 200 m (short thick red lines), together with the simultaneous mean of CIMS BrO (short thick black lines), and the 1-h smoothed CIMS BrO up to 2 h before and after the MAX-DOAS measurements (thin purple lines). The purple lines account for the MAX-DOAS sampling air centred up to 4 km away and if winds were as low as 2 km h^{-1} . Purple lines demonstrates that the lack of collocation of MAX-DOAS and CIMS measurements cannot be responsible for the apparent 10-fold discrepancy them.

[Title Page](#)[Abstract](#)[Introduction](#)[Conclusions](#)[References](#)[Tables](#)[Figures](#)[◀](#)[▶](#)[◀](#)[▶](#)[Back](#)[Close](#)[Full Screen / Esc](#)[Printer-friendly Version](#)[Interactive Discussion](#)

Resolution of a discrepancy between remote and in-situ measurements

H. K. Roscoe et al.

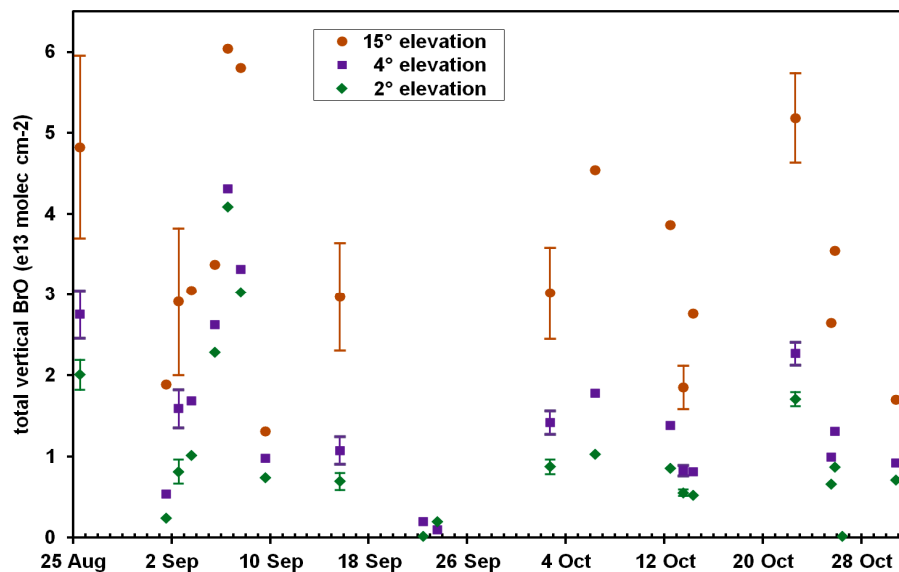


Fig. 5. Total vertical tropospheric BrO measured at Halley in Antarctica in spring 2007 by MAX-DOAS, at each elevation angle. These are medians of each sunny day or part-day. The air mass factors assume that all the BrO is in the lowest 200 m. Estimates of 1- σ error bars are shown at selected points (all error bars would overly clutter the plot), showing significant differences between the elevations on many days. Later errors are smaller due to the increasing duration of daylight.

[Title Page](#)[Abstract](#)[Introduction](#)[Conclusions](#)[References](#)[Tables](#)[Figures](#)[⏪](#)[⏩](#)[⏴](#)[⏵](#)[Back](#)[Close](#)[Full Screen / Esc](#)[Printer-friendly Version](#)[Interactive Discussion](#)

Resolution of an discrepancy between remote and in-situ measurements

H. K. Roscoe et al.

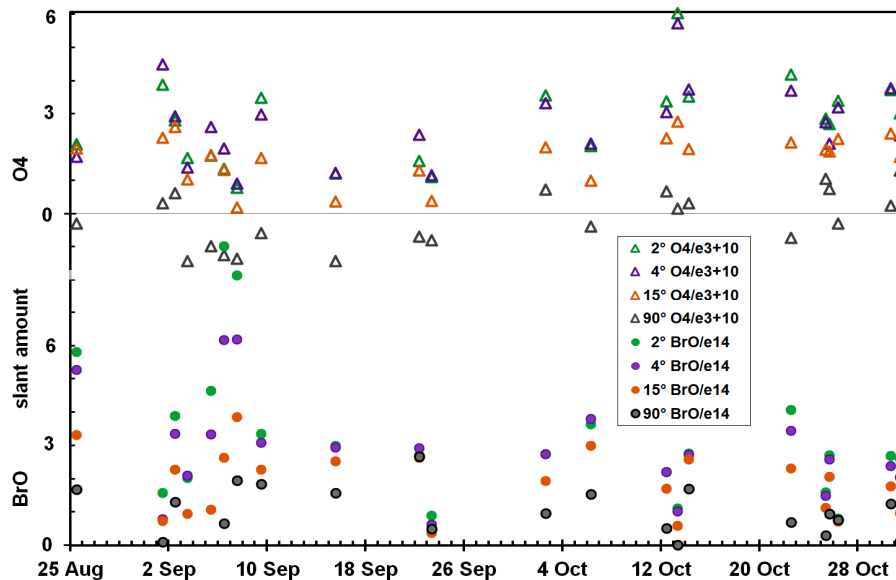


Fig. 6. Slant amounts of BrO and O₄ measured at Halley in Antarctica in spring 2007 by MAX-DOAS at the elevations observed (units as Fig. 1). These are medians of each sunny day or part-day. The reference spectrum was often on a nearby rather than the same day, hence the non-zero values at 90°.

Title Page

Abstract

Introduction

Conclusions

References

Tables

Figures

◀

▶

◀

▶

Back

Close

Full Screen / Esc

Printer-friendly Version

Interactive Discussion



Resolution of an discrepancy between remote and in-situ measurements

H. K. Roscoe et al.

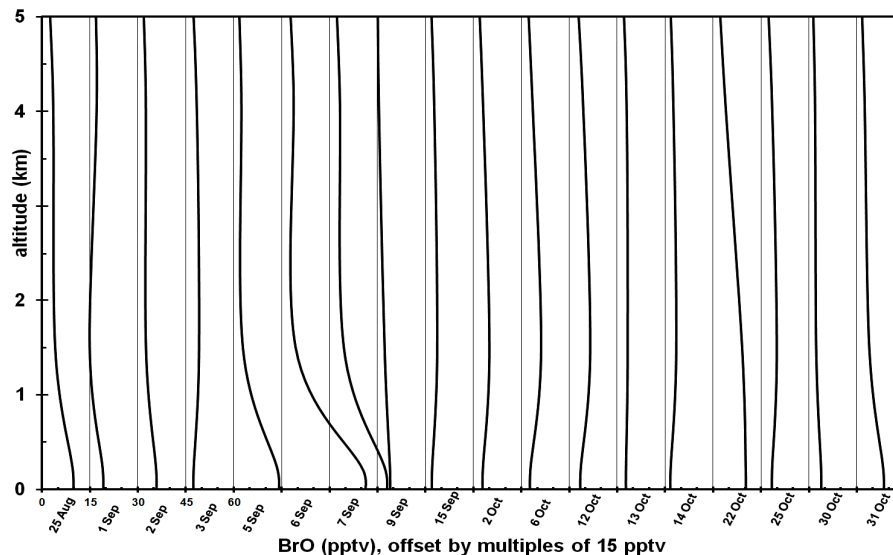


Fig. 7. Vertical profiles of BrO inverted from the MAX-DOAS data (see Sect. 5). Values have been vertically averaged over the altitude ranges for which the inversion has near-independent pieces of information, centred at 0.2, 1.5 and 4.3 km respectively, connected by smooth lines to guide the eye.

[Title Page](#)[Abstract](#)[Introduction](#)[Conclusions](#)[References](#)[Tables](#)[Figures](#)[⏪](#)[⏩](#)[◀](#)[▶](#)[Back](#)[Close](#)[Full Screen / Esc](#)[Printer-friendly Version](#)[Interactive Discussion](#)

Resolution of an discrepancy between remote and in-situ measurements

H. K. Roscoe et al.

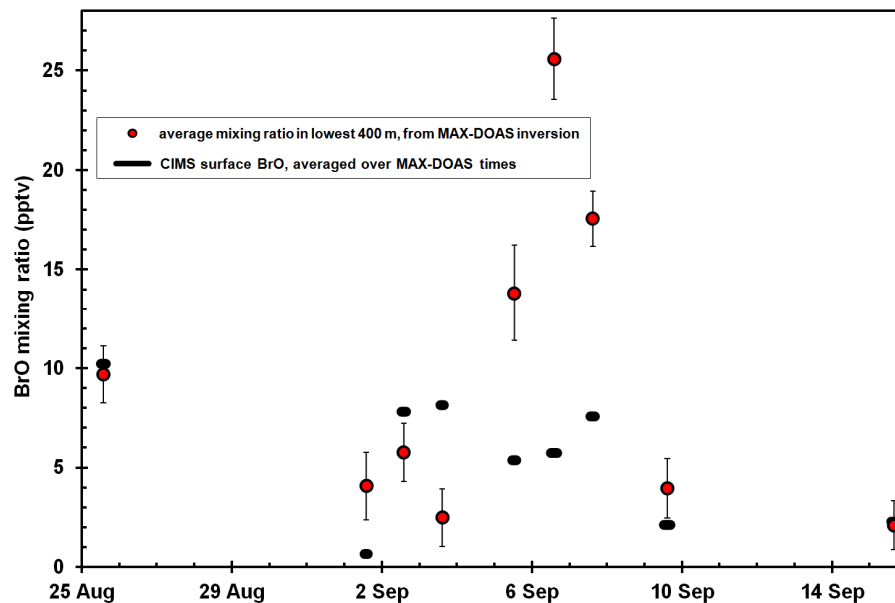


Fig. 8. Near-surface mixing ratios of BrO from the inversion of MAX-DOAS data, compared to the simultaneous in-situ measurements by the CIMS. Error bars on MAX-DOAS inversions are 1-sigma. The ratio of the mean MAX-DOAS to mean CIMS values shown here is 1.7 ± 0.6 , compared to the 10-fold disagreement in Fig. 4.

[Title Page](#)[Abstract](#)[Introduction](#)[Conclusions](#)[References](#)[Tables](#)[Figures](#)[◀](#)[▶](#)[◀](#)[▶](#)[Back](#)[Close](#)[Full Screen / Esc](#)[Printer-friendly Version](#)[Interactive Discussion](#)

Resolution of an discrepancy between remote and in-situ measurements

H. K. Roscoe et al.

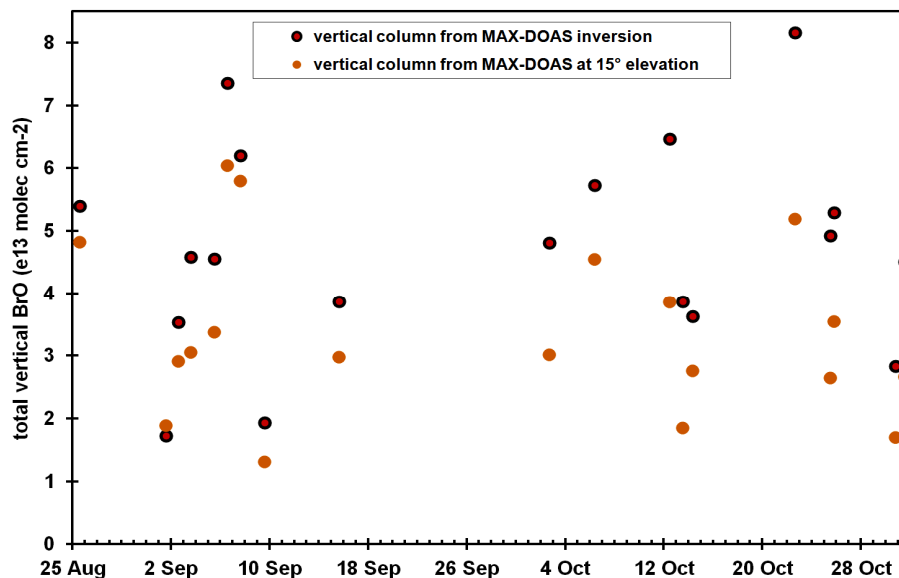


Fig. 9. Vertical amounts of BrO from the inversion of MAX-DOAS data, compared to the simple calculation of vertical amounts from the 15° elevation MAX-DOAS data. The latter values are mostly smaller, suggesting consistent errors in the AMFs, unsurprising as they assumed all BrO to be near the surface.

[Title Page](#)[Abstract](#)[Introduction](#)[Conclusions](#)[References](#)[Tables](#)[Figures](#)[⏪](#)[⏩](#)[◀](#)[▶](#)[Back](#)[Close](#)[Full Screen / Esc](#)[Printer-friendly Version](#)[Interactive Discussion](#)

Resolution of an discrepancy between remote and in-situ measurements

H. K. Roscoe et al.

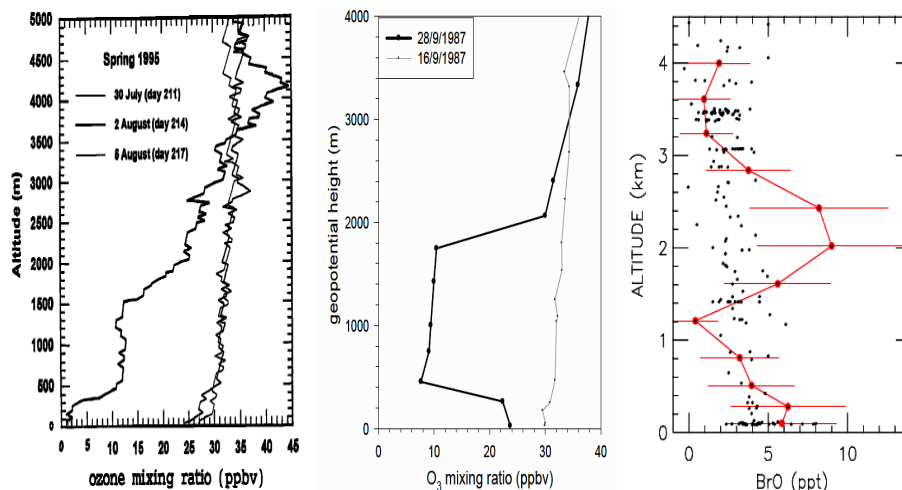


Fig. 10. Left: selected ozonesonde profiles measured in spring in Antarctica at Neumayer (71° S 8° W) in 1995 (Roscoe et al., 2001), showing ozone depletion well above the 200 to 300-m thick boundary layer on one of the days. Centre: as left but at Halley in 1987 (Jones et al., 2010). Right: BrO profiles measured in the Arctic on an aircraft flight in spring 2008, showing (red) BrO well above the boundary layer during an enhancement episode, and (black dots) parts of the flight with more modest enhancements (Salawitch et al., 2010).

[Title Page](#)[Abstract](#)[Introduction](#)[Conclusions](#)[References](#)[Tables](#)[Figures](#)[◀](#)[▶](#)[◀](#)[▶](#)[Back](#)[Close](#)[Full Screen / Esc](#)[Printer-friendly Version](#)[Interactive Discussion](#)